

THE GEORGE
WASHINGTON
UNIVERSITY

WASHINGTON, DC



M

n

In
E

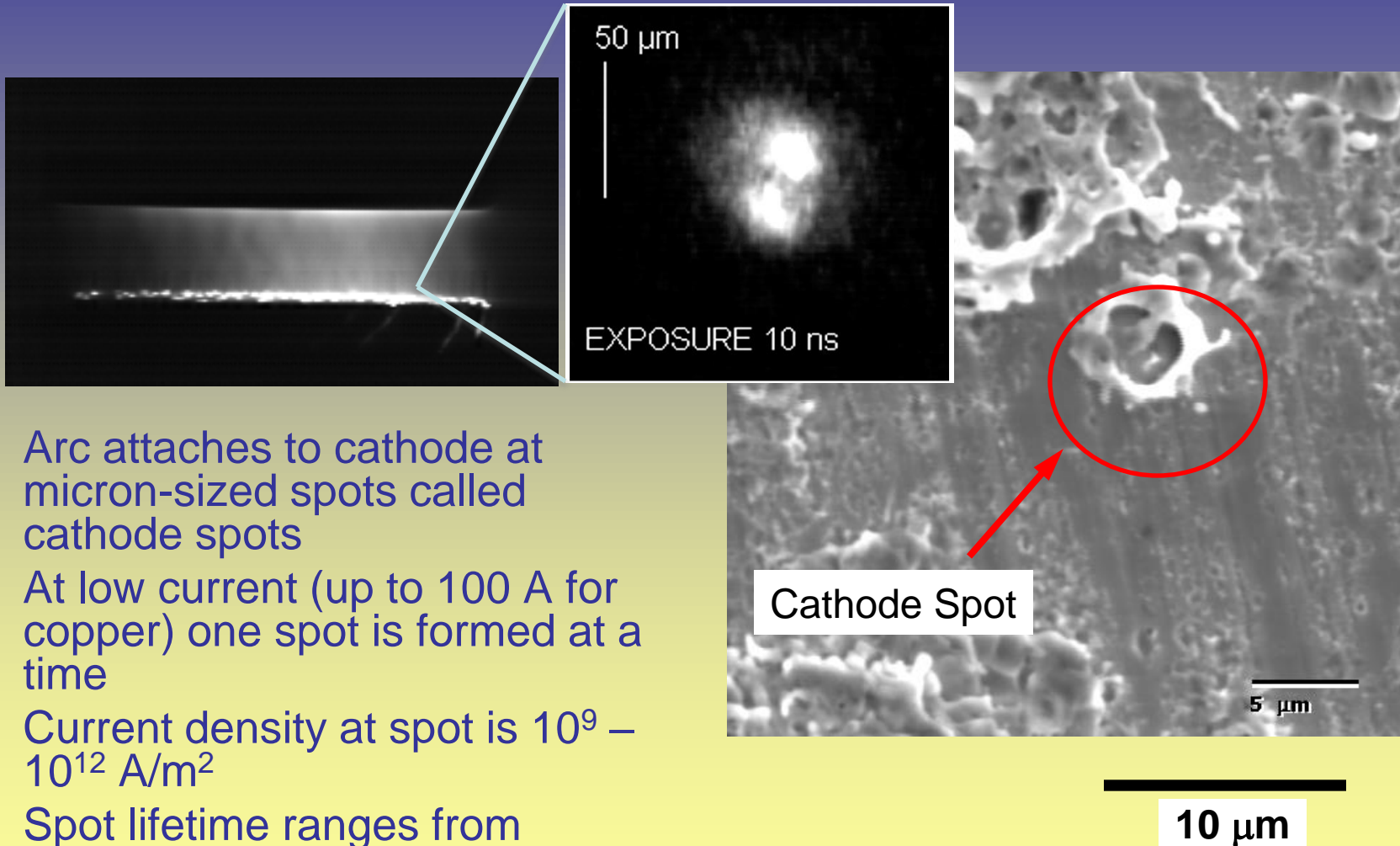
Ackno

Micropropulsion and Nanotechnology Laboratory (MPNL)

Smartphone summary:

vacuum arc plasmas are quite complicated
thus multiple approaches are required

Vacuum Arc



- Arc attaches to cathode at micron-sized spots called cathode spots
- At low current (up to 100 A for copper) one spot is formed at a time
- Current density at spot is $10^9 - 10^{12}$ A/m²
- Spot lifetime ranges from nanoseconds to microseconds

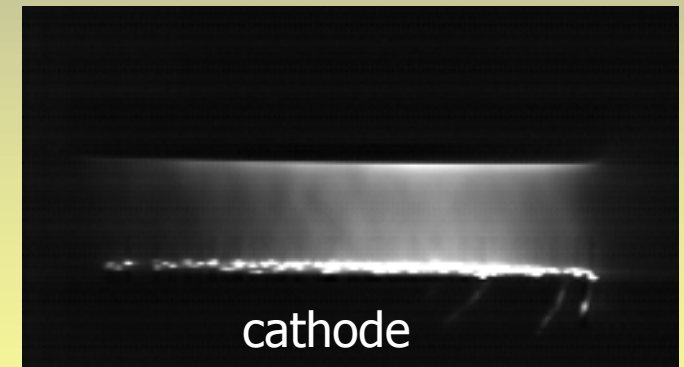
High Arc Current Vacuum Arc

- >1 kA
- Transition to the diffuse mode
 - Magnetic field effect
- Plasma model
 - Expansion of individual cathode jets
 - Formation of common channel from overlap
 - Single jet in the presence of high-current column (imposed voltage on single jet) and magnetic field

Columnar arc



Diffuse arc



The Free Boundary Model

$$m_i(\mathbf{v}_i \cdot \nabla)\mathbf{v}_i = -k(Z_i T_e + T_i) \frac{\nabla n}{n} + \frac{\mathbf{j} \times \mathbf{B}}{n}$$

$$\mathbf{j} = \sigma \left(\mathbf{E} + \frac{kT_e}{e} \frac{\nabla n}{n} - \frac{\mathbf{j} \times \mathbf{B}}{en} + \mathbf{v}_i \times \mathbf{B} \right)$$

$$\nabla \cdot (n\mathbf{v}_i) = 0$$

$$\nabla \cdot \mathbf{j} = 0$$

$$\mathbf{E} = -\nabla \phi$$

$$\frac{3}{2} k N_e V \nabla T_e + 3 \frac{j_e}{e} k \nabla T_e + k T_e \operatorname{div}(j) = -P_e \operatorname{div}(V) + \frac{j^2}{\sigma}$$

$$B_\theta(r) = \frac{\mu_0}{r} \int_0^r j_z r' dr'$$

$$\frac{\partial \alpha}{\partial \tau} = \frac{1}{1 + \left(\frac{V_n}{V_\tau}\right)^2} \cdot \frac{\frac{\partial V_n}{\partial \tau} V_\tau - \frac{\partial V_\tau}{\partial \tau} V_n}{V_\tau^2}$$

- Assumptions

- Steady-state, fully ionized, collision dominated, quasi-neutral plasma
- Anode acts as a passive current and particle collector
- Cathode spots act as source of plasma at a specified jet angle and velocity
- Cathode spots evenly distributed (no arc constriction) within a circular area
- Magnetized electrons, unmagnetized ions
- External magnetic field purely axial and uniform, self field purely azimuthal

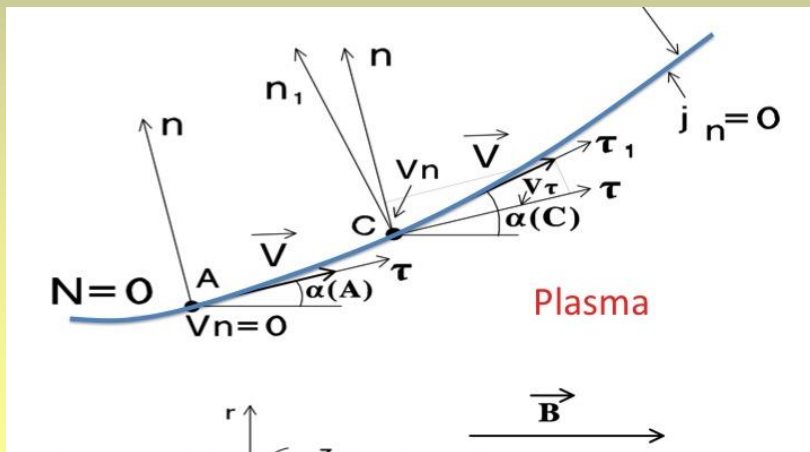
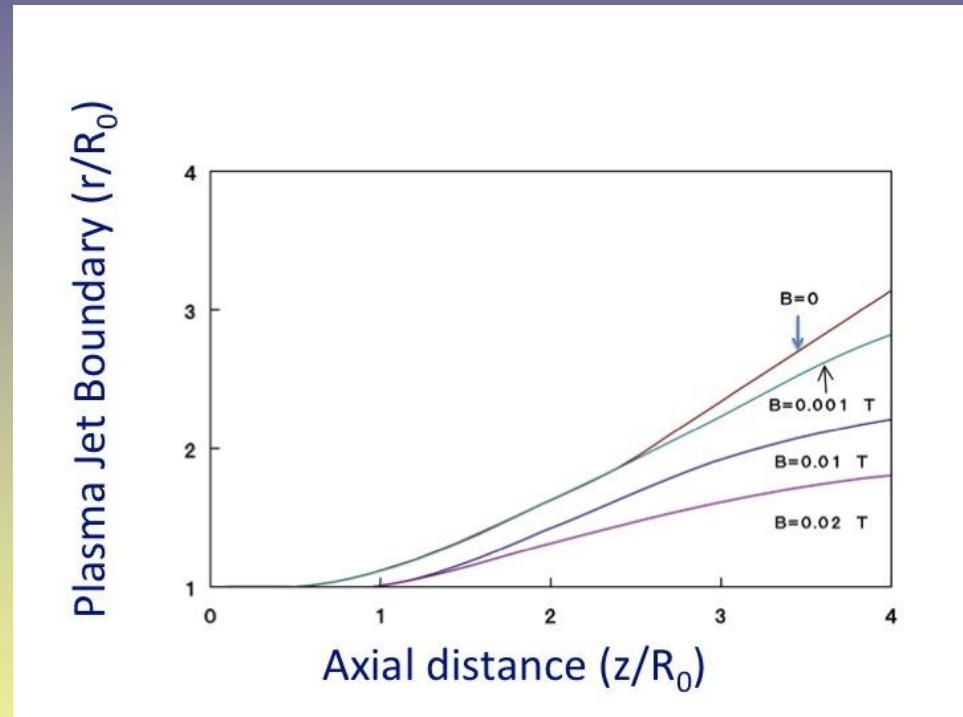
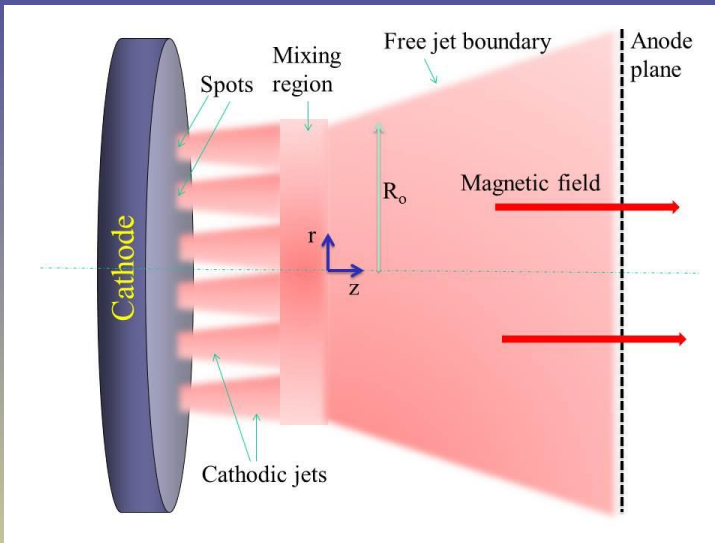
- Numerical methods

- Iterative scheme for solving for the potential
- Implicit second-order accuracy method to calculate the velocity, current density, and density from the potential

- Two approaches:

- self consistent solution
- voltage is set by high-current column

Free plasma jet boundary

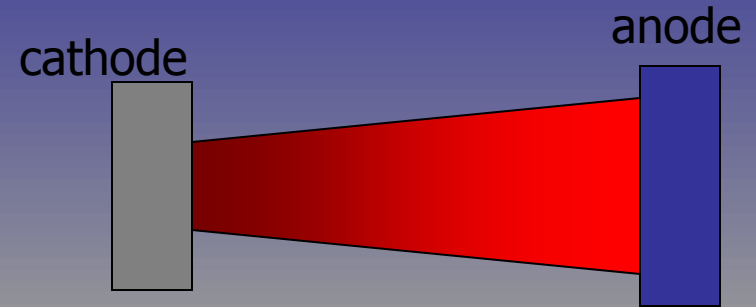
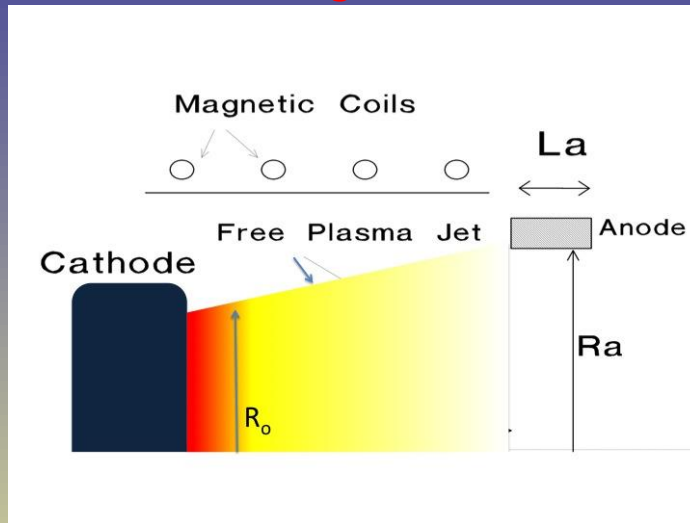


M. Keidar et al, *J. Phys. D*, 1996

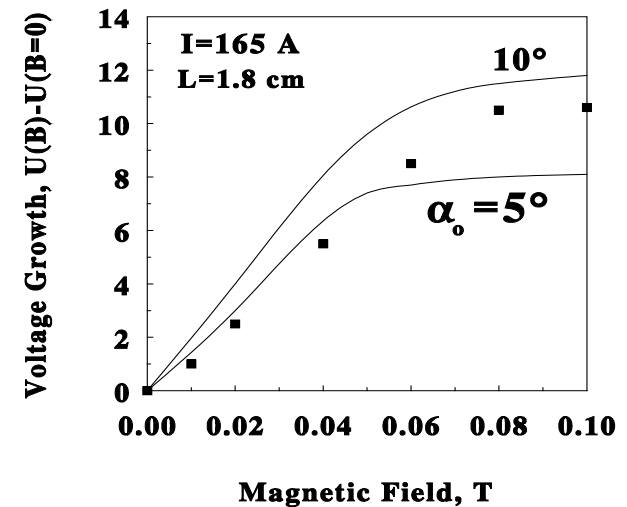
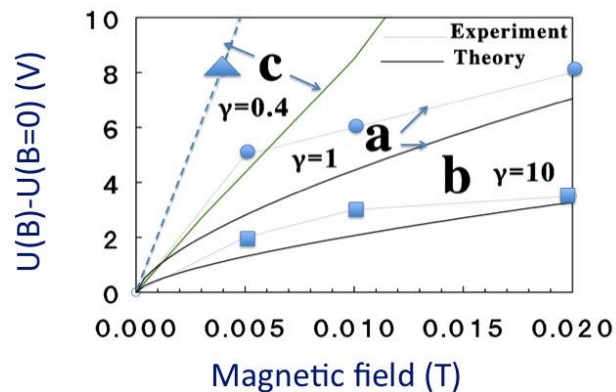
M. Keidar and I. I. Beilis, *Plasma Engineering*, Elsevier, 2013

Focusing and Arc Voltage

Ring anode

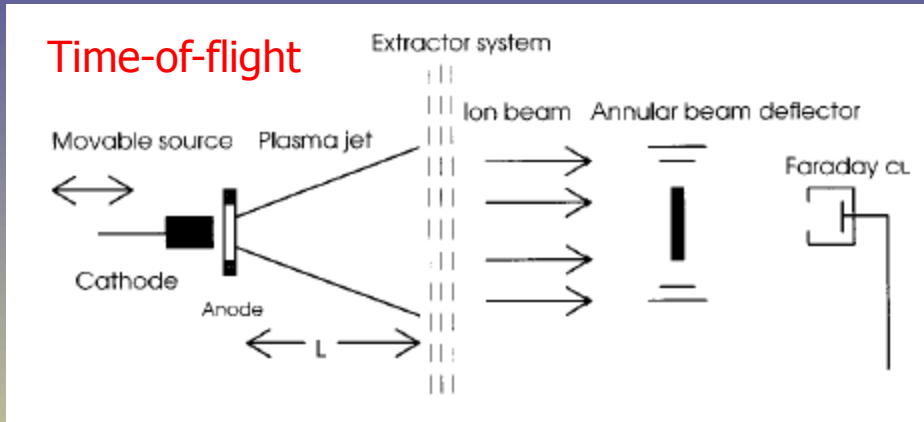


Disk anode

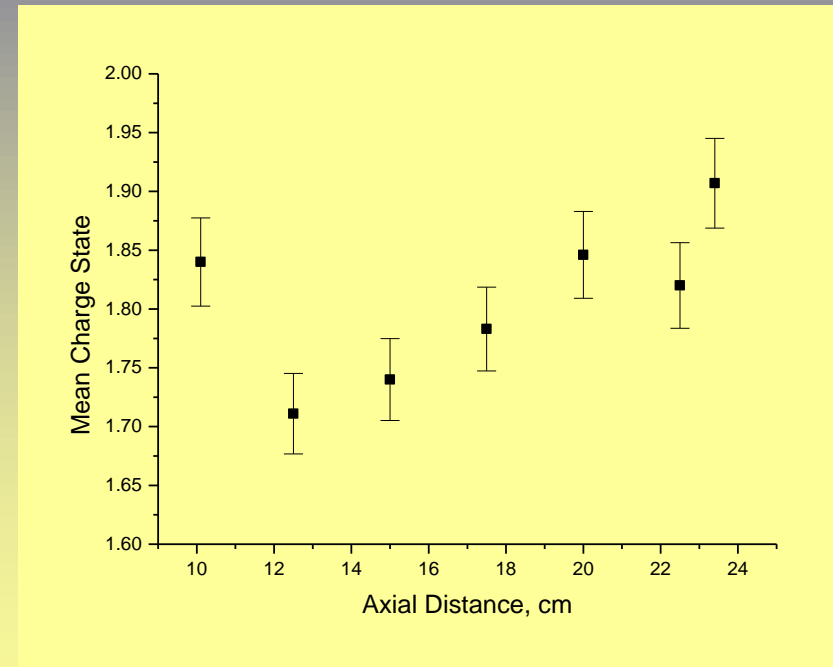
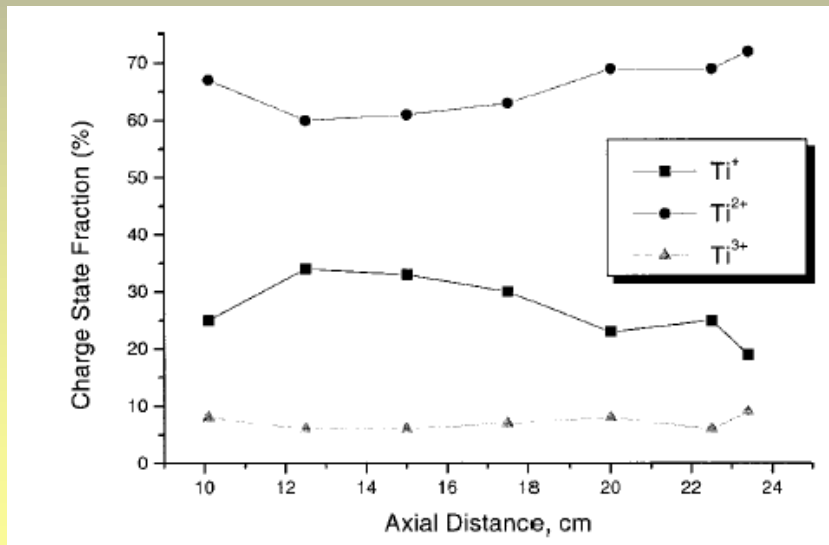


Multiply charged ion transport

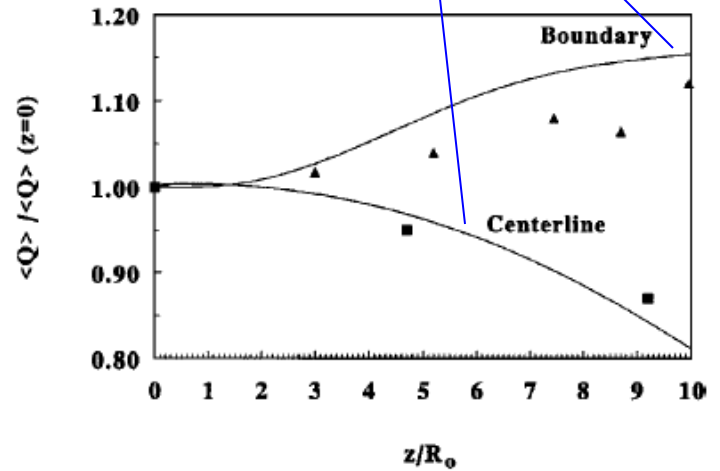
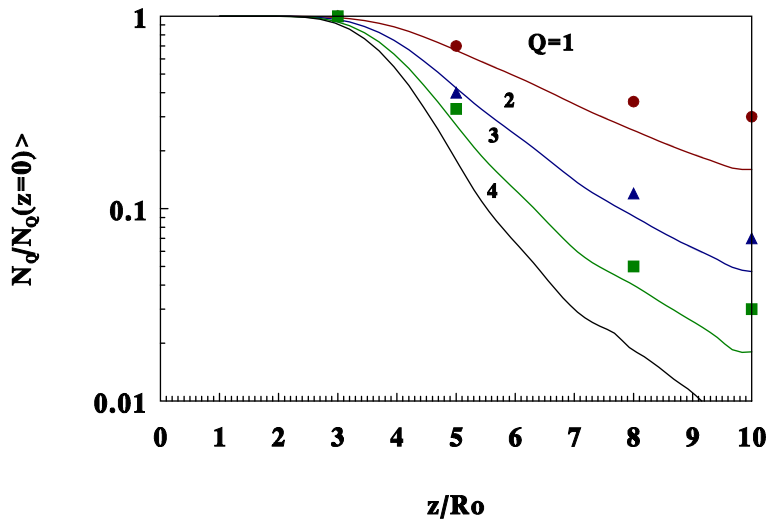
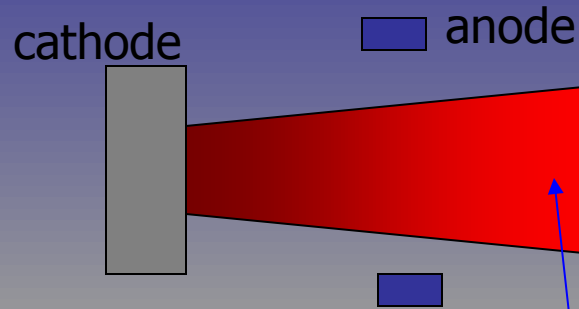
Mean ion charge state generally >1



Mean Charge along the jet

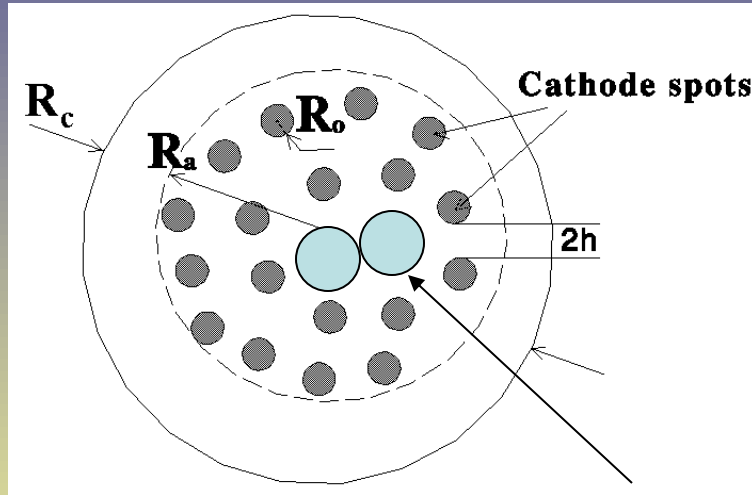


Comparison with Experiment



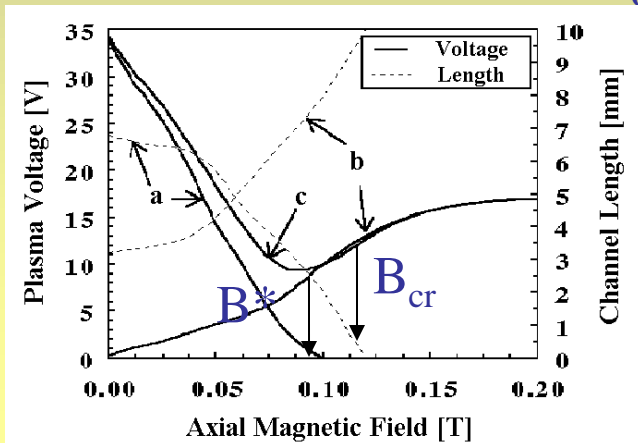
Experiment: V.M. Khoroshikh,
Sov. Phys. Tech. Phys., 33(6)
723 (1988)

Condition for critical AMF



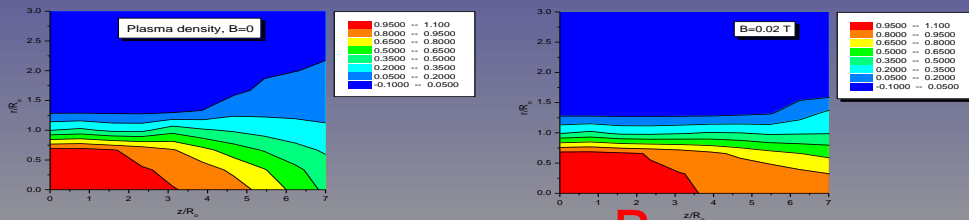
$$R_o + \Delta r_{jet}$$

- $\Delta r_{jet}(L, B_{cr}) = h(I_{arc}, R_a)$
- L is the gap length
- $\Delta r_{jet}(L, B)$ is the increase of the plasma jet radius due to the radial expansion
- $2h(I_{arc}, R_a)$ is the distance between two individual adjacent channels

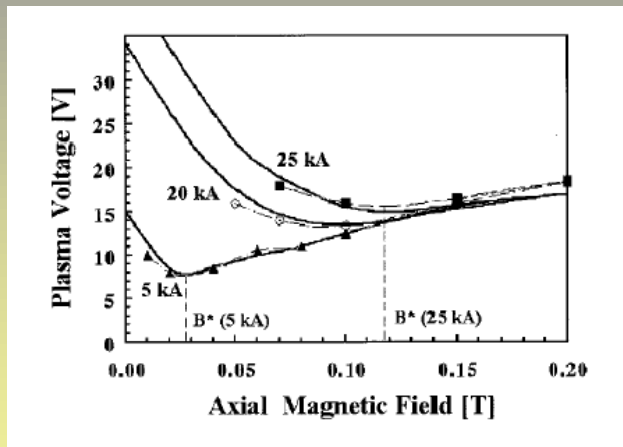


Columnar & Diffuse Arc in a Magnetic Field

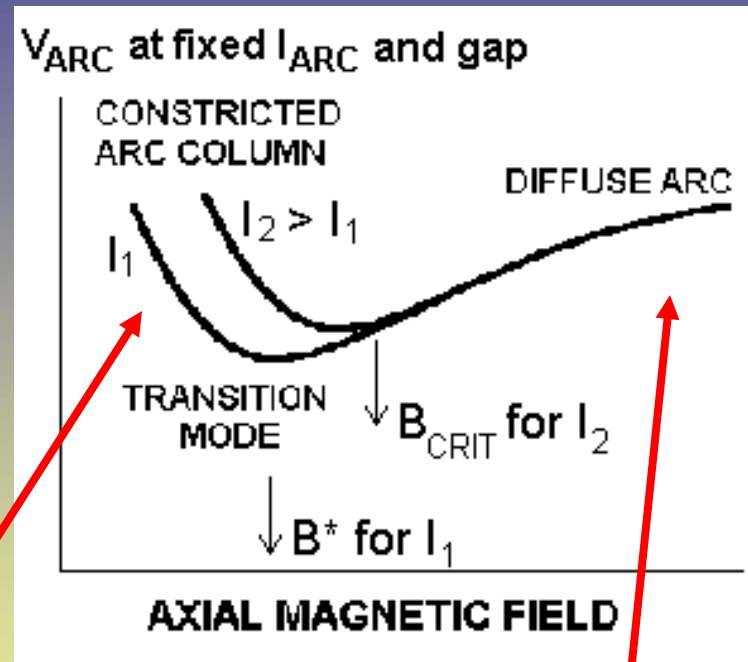
Plasma density



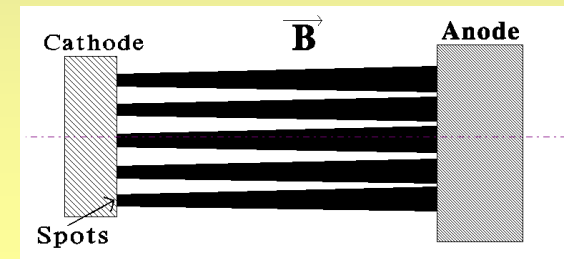
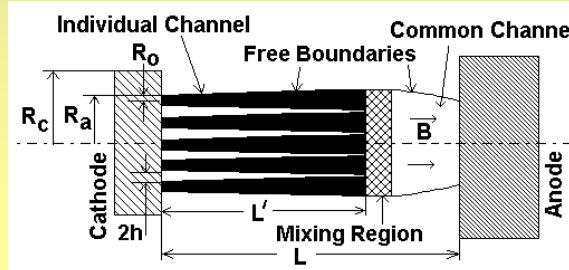
Model prediction



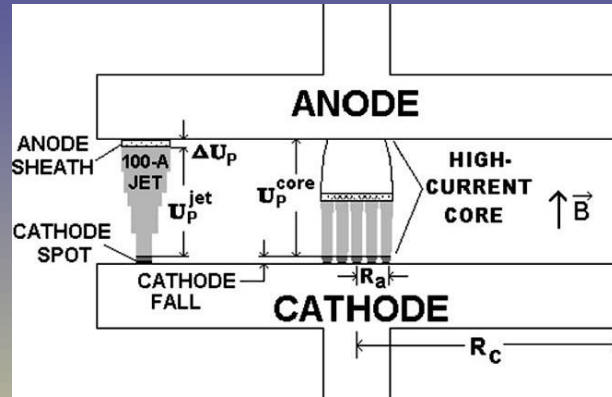
V-shape voltage characteristic



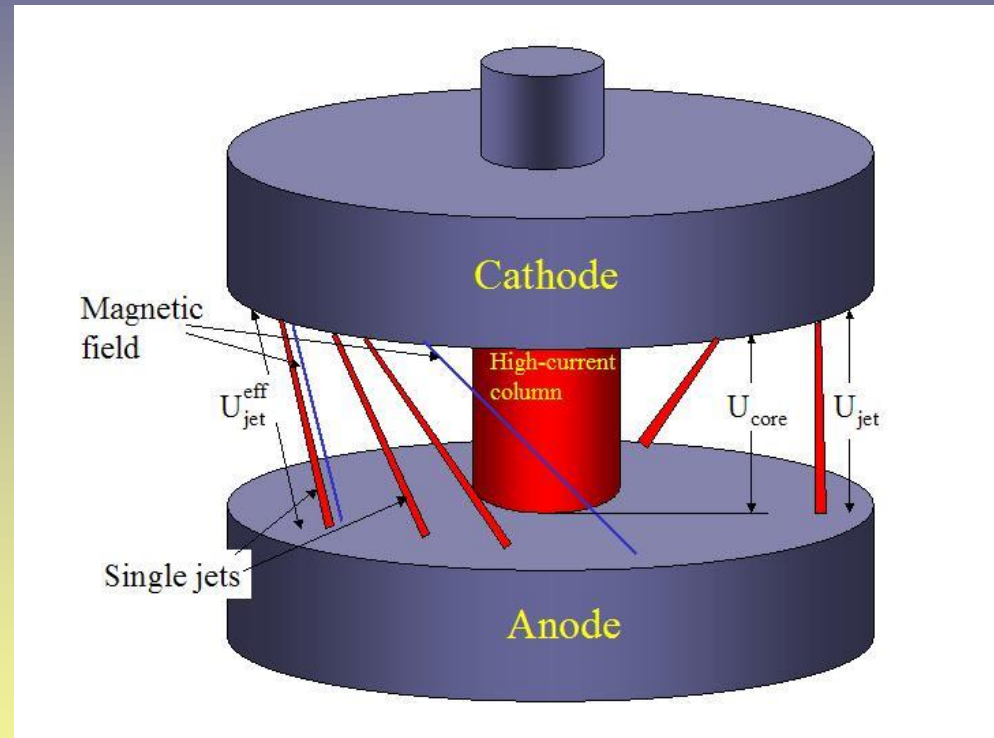
Gundlach, *ISDEIV*, 1972



High-current vacuum arc



- Two-dimensional free expansion of the plasma jets
- Voltage is calculated for the individual jets and high-current column
- *Diffuse column arc*: Expansion of single cathodic jet burning in parallel to high current column



Anode sheath potential drop

Anode sheath potential drop

Anode sheath potential drop

$$\Delta\phi = T_e \ln[j_{th}(r,z)/j(r,z)]$$

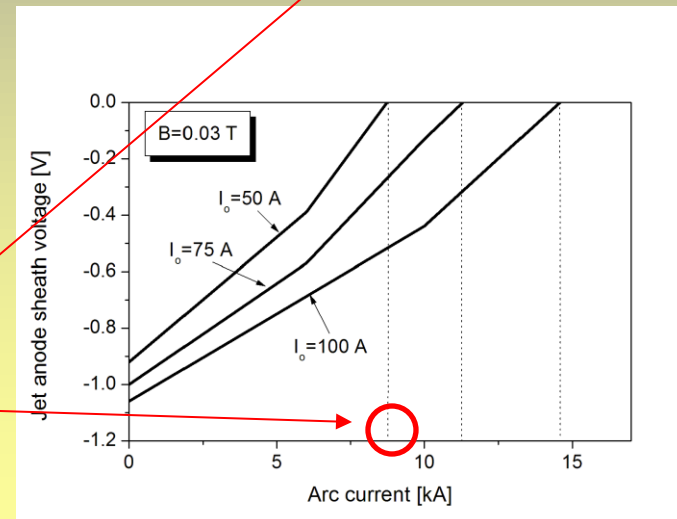
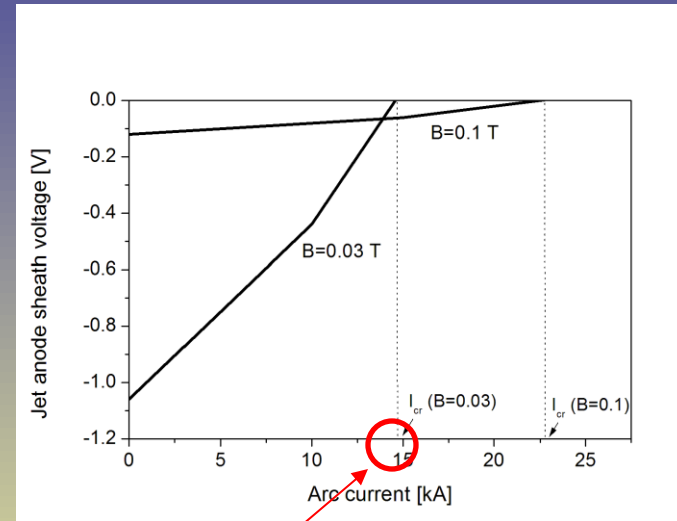
- $j_{th}(r,z)$ electron thermal current depends on density
- $j(r,z)$ current density

Single jet existence criteria

$$\Delta\phi = 0, I = I_{cr}$$

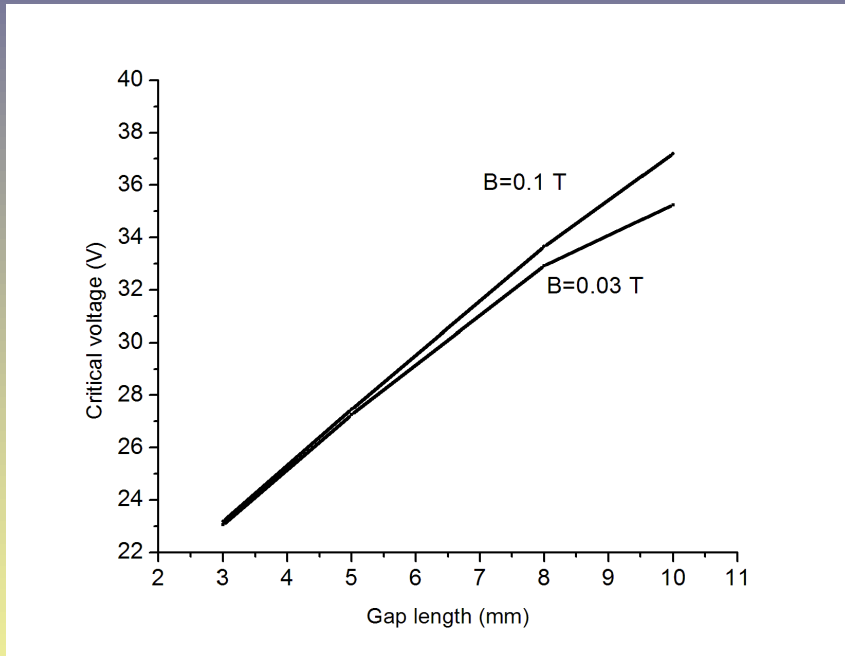
- $I > I_{cr}$ the isolated jet extinguishes
- $I < I_{cr}$ the isolated jet is stable, which is characteristic of diffusing arcs

Critical arc current

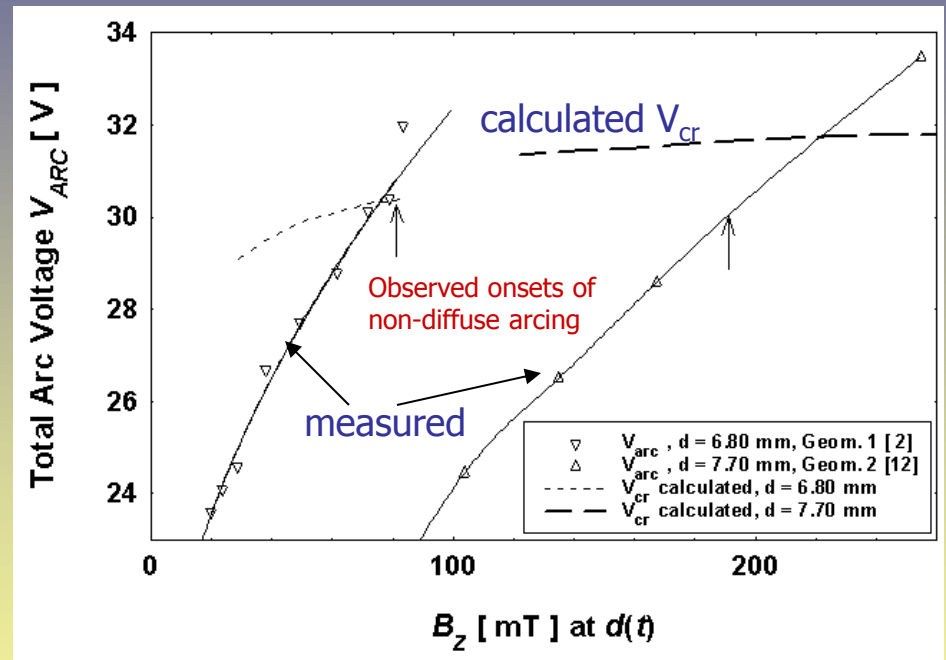


Critical voltage

Critical voltage as a function of gap length



Comparison with experiment



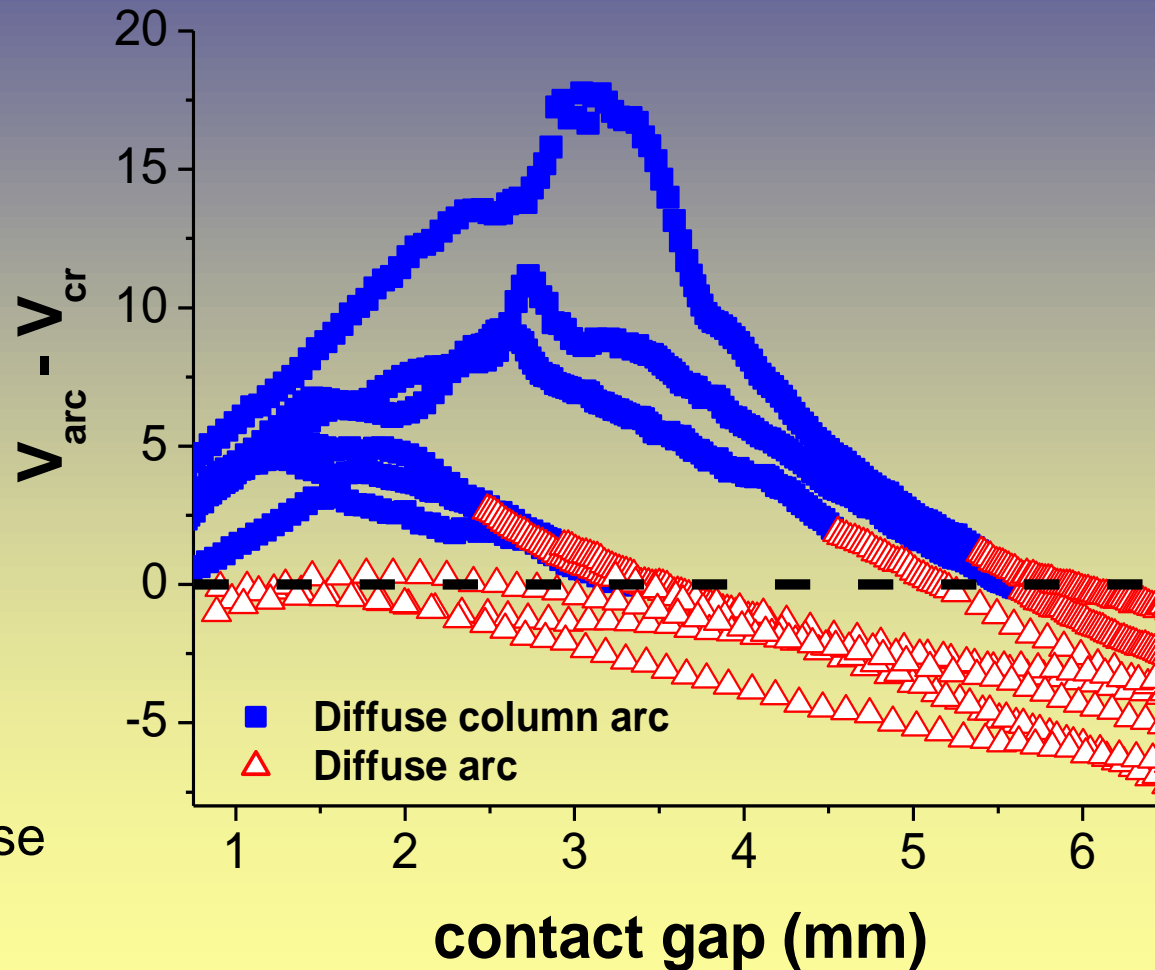
$V_{arc} < V_{cr}$ – is diffuse arc condition

Experiment

M. B. Schulman and H. Schellekens, 2000

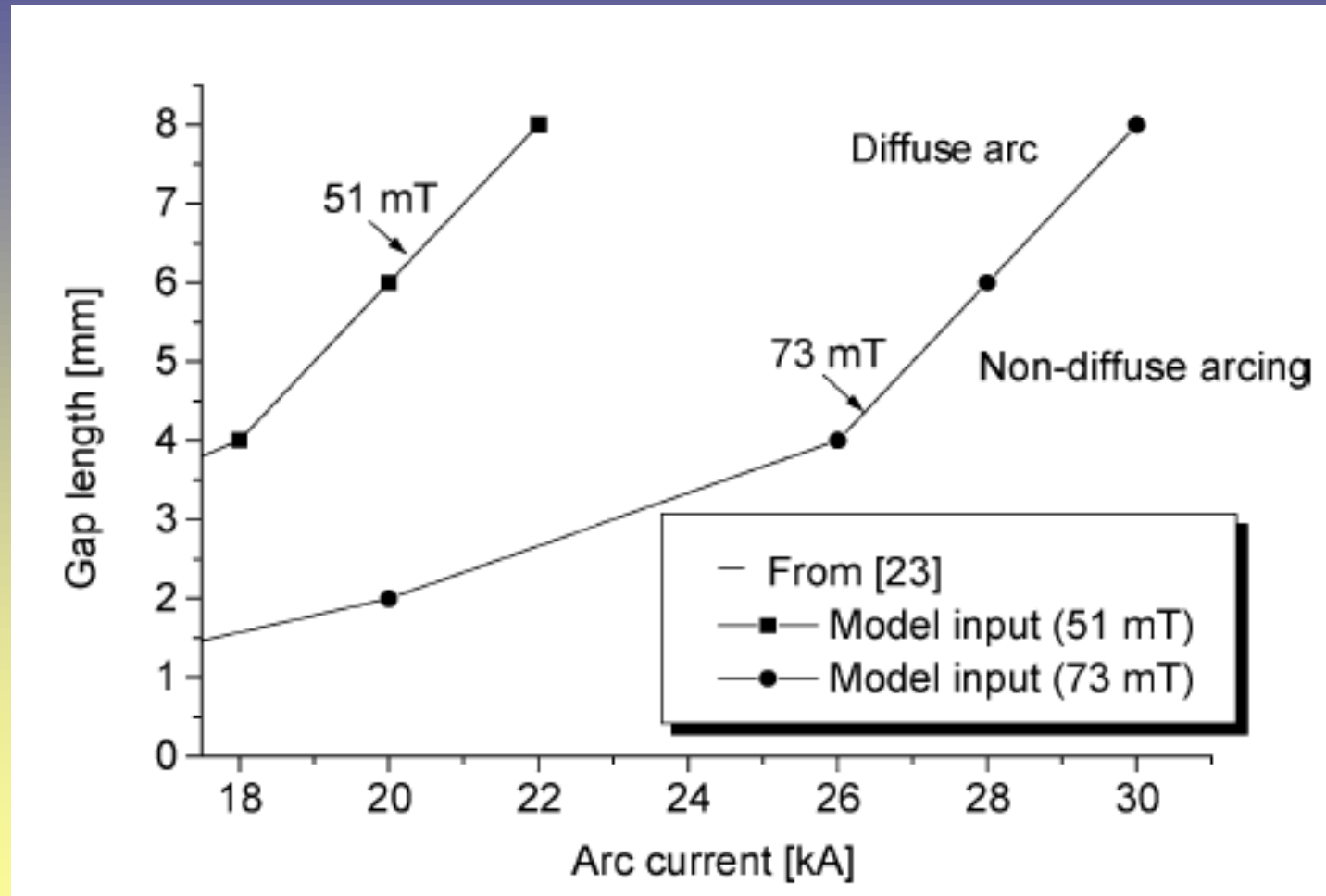
Keidar et al, *IEEE Trans. Plasma Sci*, 2004

Comparison with experiment



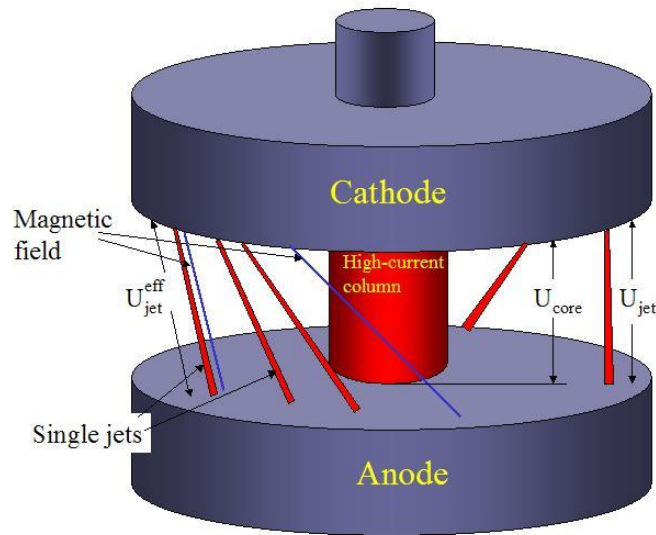
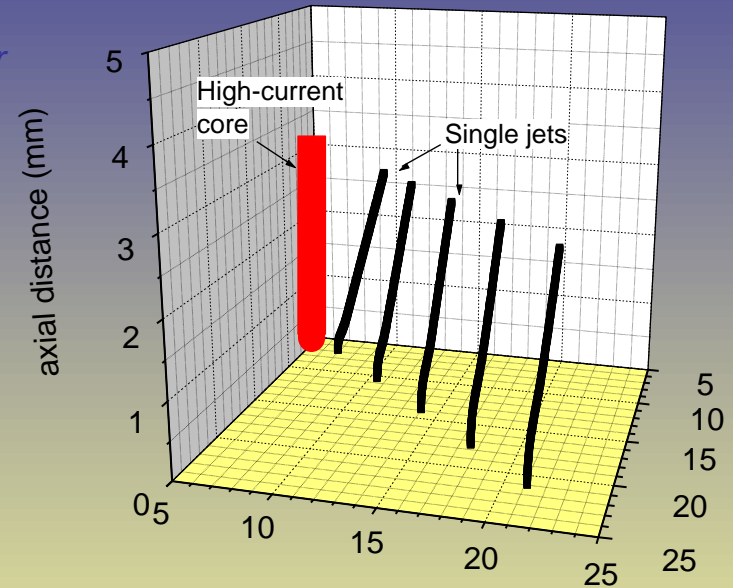
$V_{\text{arc}} < V_{\text{cr}}$ – is diffuse arc condition

Diagram of Modes



Arc Voltage Criterion

- Single jets appear even when $V_{arc} > V_{cr}$
- Single jet appearance is common phenomenon during evolution into a high-current diffuse arc
- More general criterion is required based on effective voltage

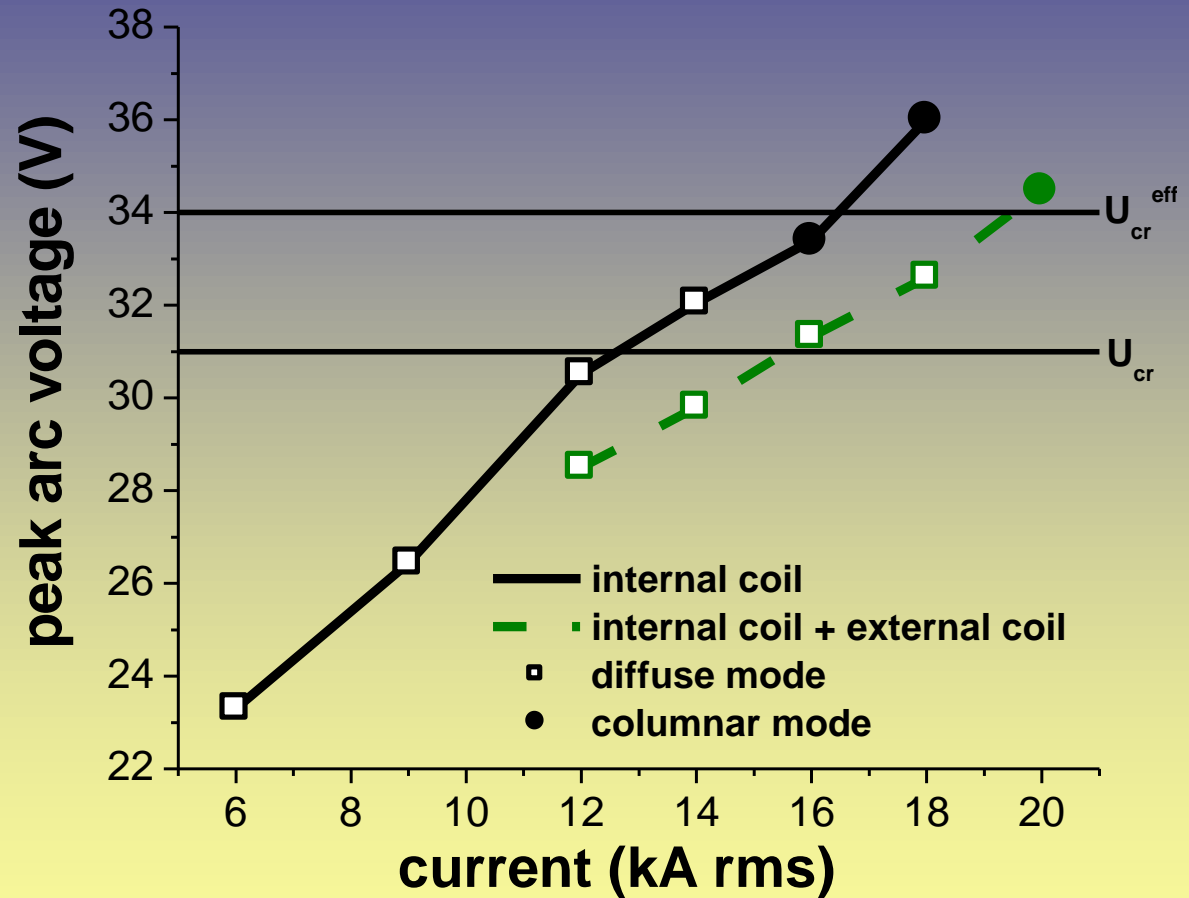


$$U_{jet}^{eff} = \int_0^{l_{eff}} E(\lambda) d\lambda$$

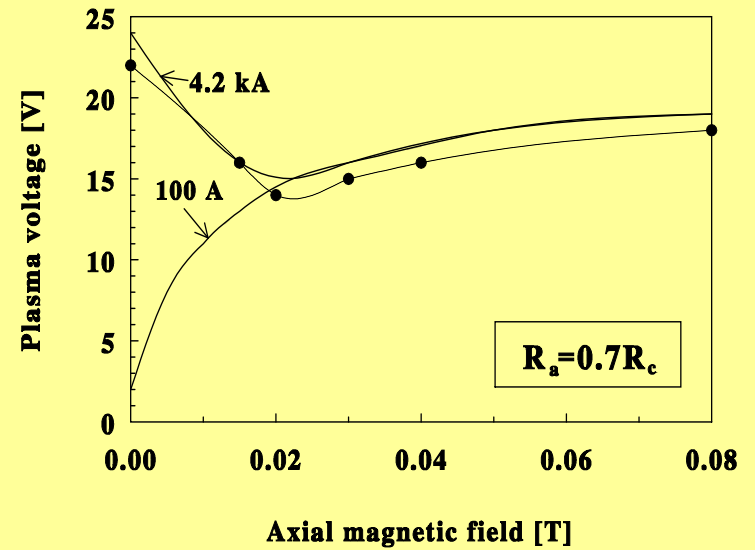
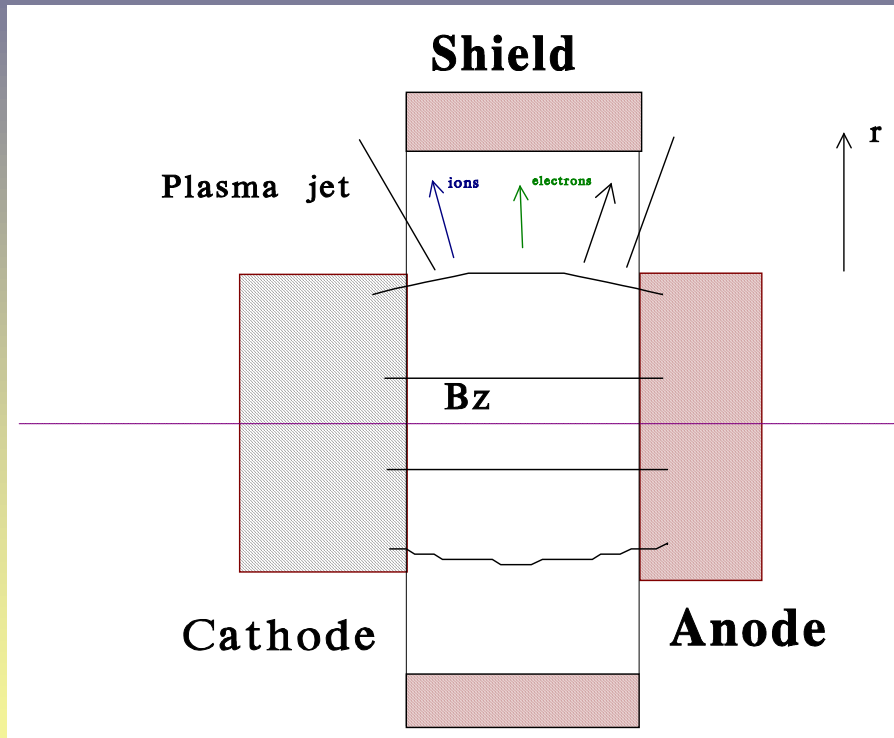
$$U_{cr}^{eff} \geq U_{arc} \geq U_{jet}^{eff}$$

Comparison with experiment

Generalized condition agrees better with observations



Radial plasma flow



The model

Similar to the model of the interelectrode gap

- hydrodynamic
- multicomponent plasma
- ambipolar flow

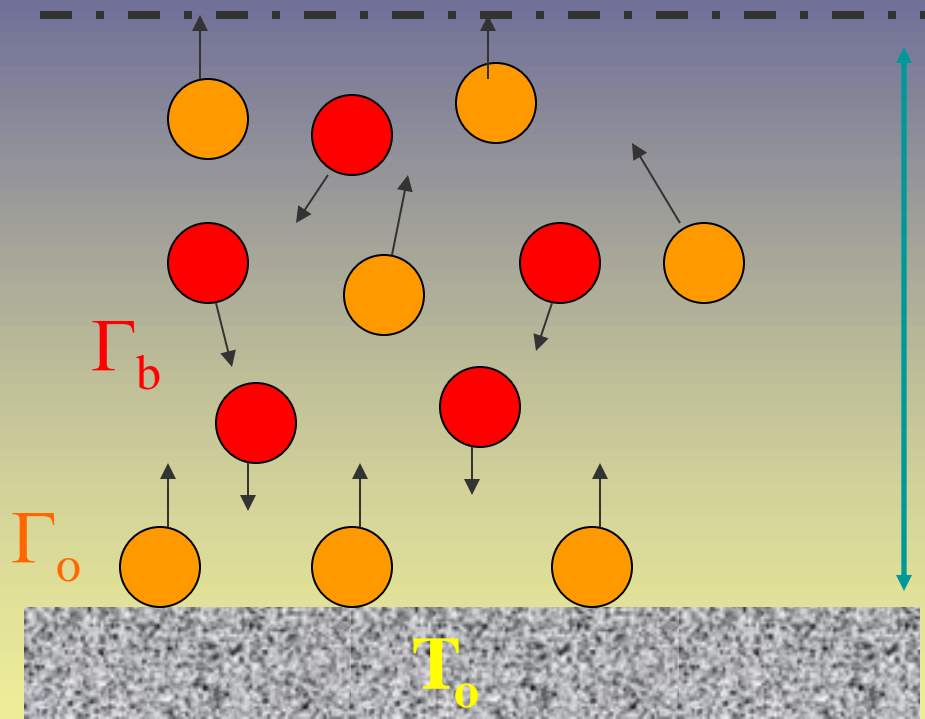
Potential distribution:

$$dU/dr = kT_e/e \cdot \nabla \ln(\sum Z_j n_j) + B \beta_e (\sum Z_j n_j V_j / \sum Z_j n_j)$$

Density
gradient

Magnetic
Field

Material ablation: non-equilibrium layer



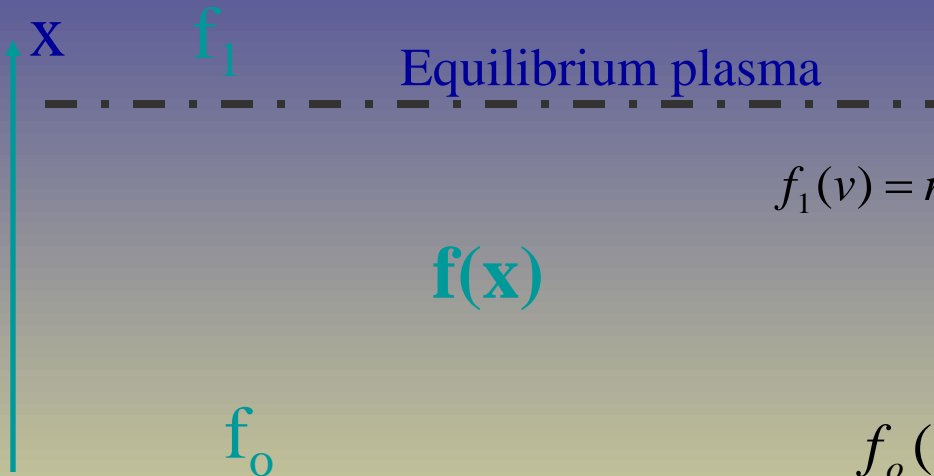
Existing models (Langmuir) can describe only low pressure <1 torr cases

Knudsen layer
~few mean free paths

The back flux Γ_b is generated due to collisions

$$\text{Evaporation flux: } \Gamma_{ev} = \Gamma_o - \Gamma_b$$

Non-equilibrium layer



Boundary conditions

$$f_1(v) = n_0 \left(\frac{m}{2\pi k T_w} \right)^{3/2} \exp\left(-\frac{m((V_x - U)^2 + V_y^2 + V_z^2)}{2k T_w} \right)$$

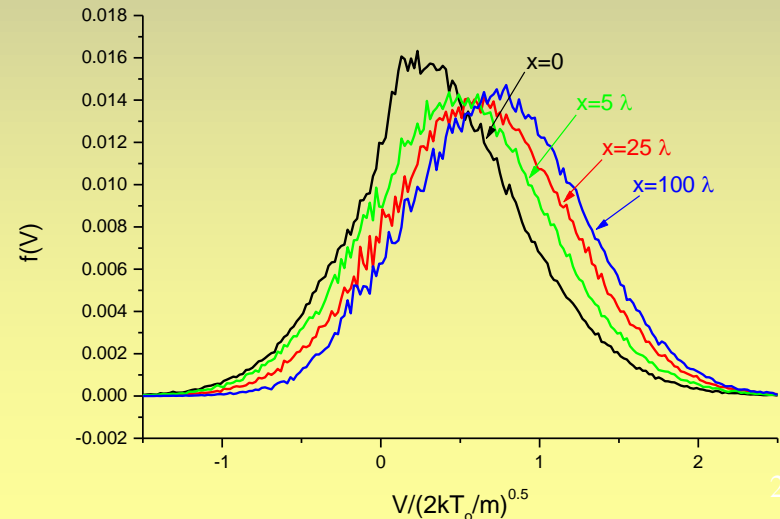
$$f_0(v) = n_0 \left(\frac{m}{2\pi k T_w} \right)^{3/2} \exp\left(-\frac{m V^2}{2k T_w} \right)$$



$$\int V_x f(V) dV = \text{const} \quad (\text{mass})$$

$$\int V_x^2 f(V) dV = \text{const} \quad (\text{momentum})$$

$$\int V_x V^2 f(V) dV = \text{const} \quad (\text{energy})$$



Kinetic model of the Knudsen Layer

Analytical and particle (DSMC) approaches:

$$f(x, \mathbf{V}) = \xi(x)f_1(\mathbf{V}) + (1 - \xi(x))f_2(\mathbf{V})$$

where $\xi(x=0)=1$ and $\xi(L)=0$ with $x=0$

[Mott-Smith, 1951]

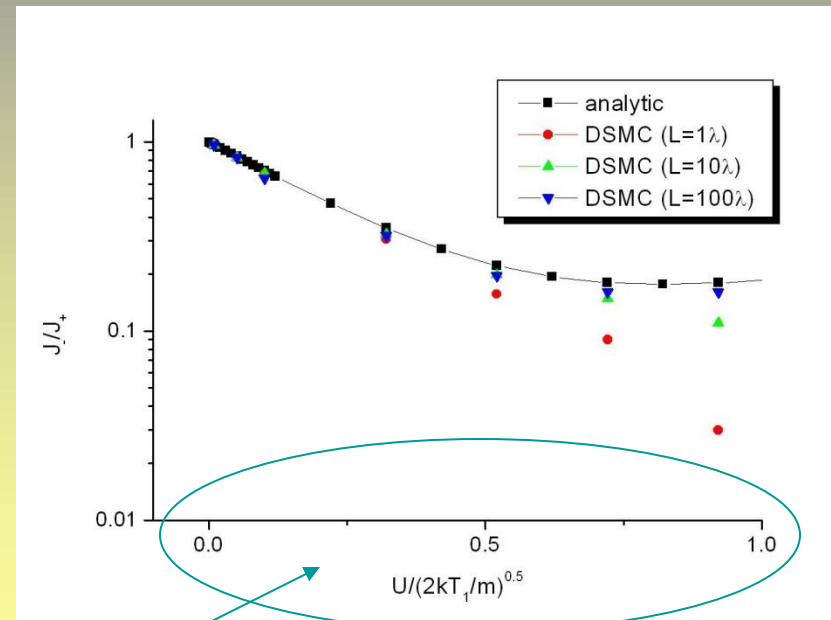
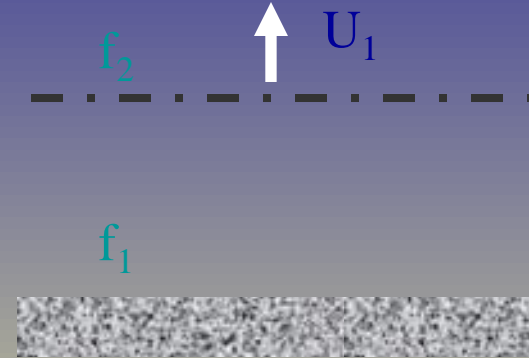
$$f_1(\mathbf{V}) = n_0 \beta^{3/2} \exp(-V^2) \quad V_x > 0$$

$$f_1(\mathbf{V}) = \delta f_2(\mathbf{V}) \quad V_x < 0$$

$$f_2(\mathbf{V}) = n_1 \beta^{3/2} \exp(-(v-U)^2)$$

[Anisimov, 1968]

Sound speed is assumed !



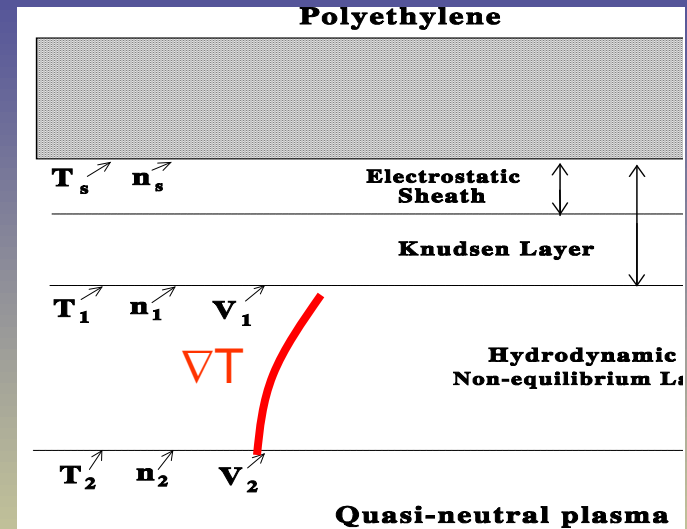
Depends on velocity

Thermal conductivity

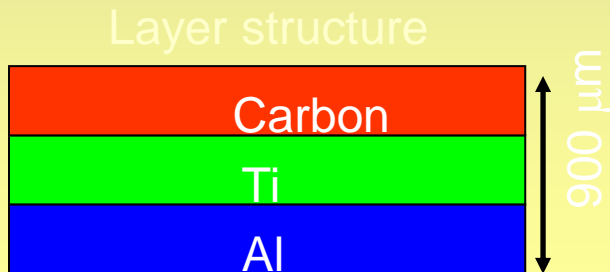
Kinetic model of Knudsen layer: effect of thermal conductivity

VDF in plasma

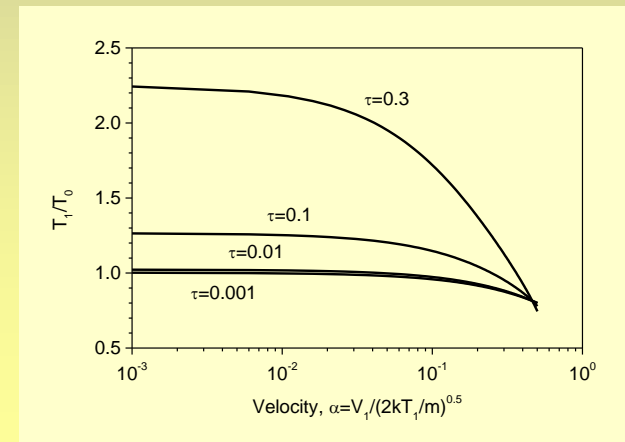
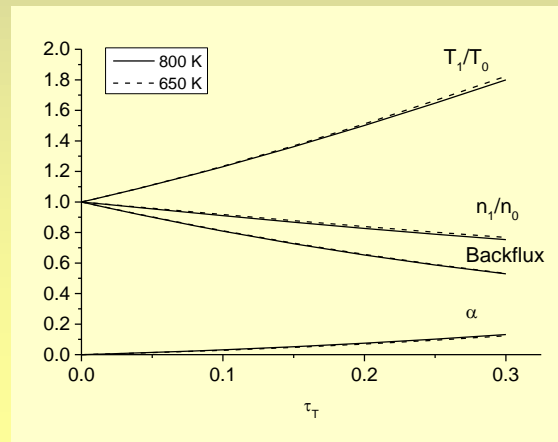
$$f_u(\vec{V}) = n_1 \cdot f_M(\vec{V}) \cdot \left\{ 1 - \frac{V_T \cdot V_1}{\nu} \cdot \left[\frac{(V_x - u)}{V_1} \cdot \left(\frac{(V_x - u)^2 + V_y^2 + V_z^2}{V_1^2} - \frac{5}{2} \right) \cdot \frac{d}{dx}(\ln T) + 2 \cdot \left(\frac{2 \cdot (V_x - u)^2 - V_y^2 - V_z^2}{3 \cdot V_1^2} \right) \cdot \frac{du}{dx} \right] \right\}$$



Effect of thermal conductivity



Pekker, Keidar *et al.*, J. Appl. Phys., 2008



Keidar *et al.*, J. Appl. Phys., 2001, 2004

Hydrodynamic Layer

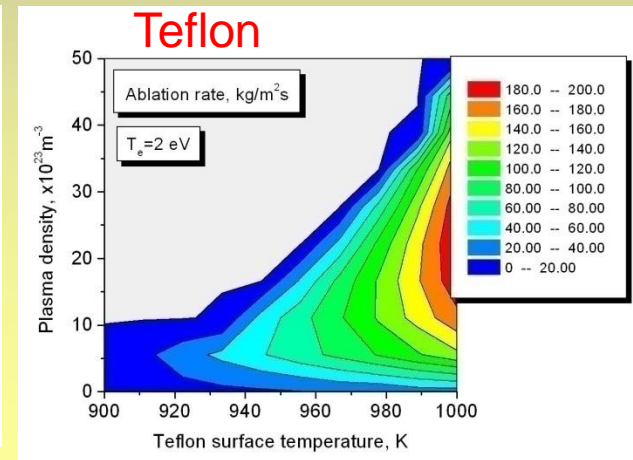
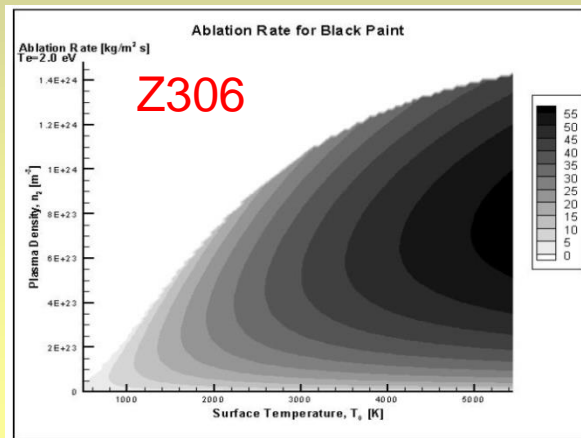
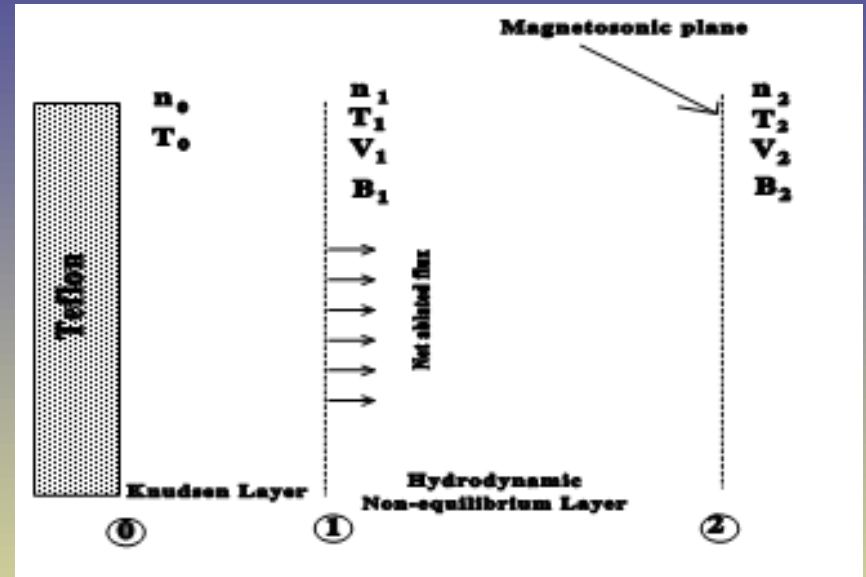
$$\nabla \cdot (nV) = \beta_{ioniz}$$

$$M(V \cdot \nabla V) = -\nabla P + j \times B$$

1D limit

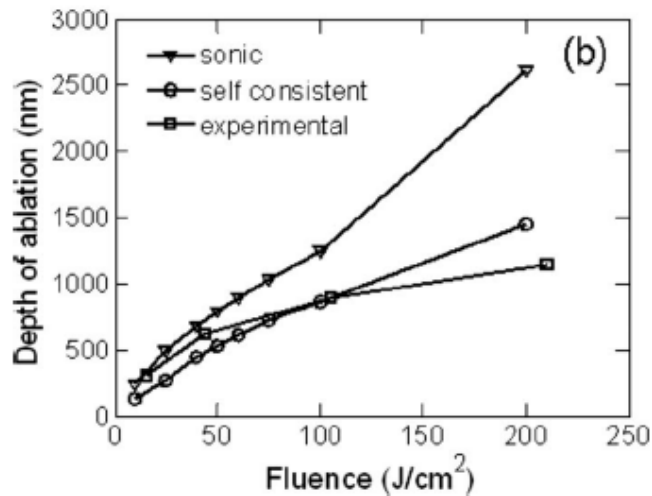
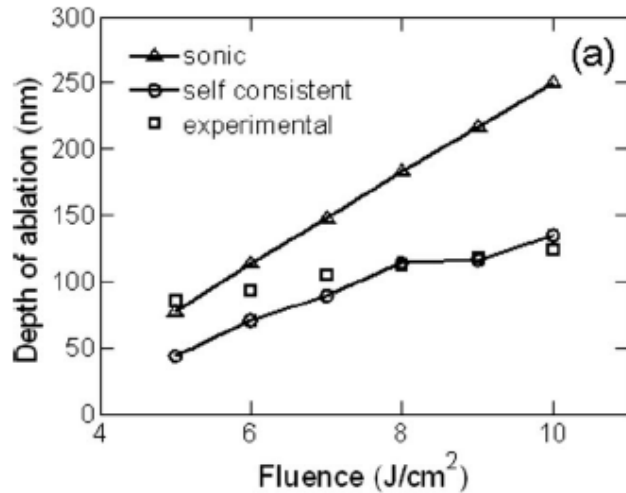
$$\frac{MU_1^2}{2kT_1} = \frac{\frac{n_1}{2} - \frac{T_2 n_2}{2T_1} + \frac{1}{4} \cdot \frac{\mu(jd)^2}{kT_1}}{\frac{3}{2} \cdot \frac{n_1^2}{n_2} - n_1}$$

U_1 depends on the specifics of acceleration (n_2, j)



**Why and where
this interactions
are important ?**

Model validation-directed energy



- Al alloy

Pulse duration 15 ns, $\lambda = 308$ nm,
Fluence 1-10 J/cm²

Dou et.al., IEEE J. Quantum
Electron. **6**, 689 2000

- Cu

Pulse duration 6 ns, $\lambda = 532$ nm,
Fluence 10-200 J/cm²

Semerok et.al., Laser Part. Beams
20, 67 2002

Predicting charring

Ablation rate

$$\Gamma = mn_1 \sqrt{\frac{1}{m} \cdot \frac{(kn_2T_2 - kn_1T_1)}{(n_1 - \frac{n_1^2}{n_2})}}$$

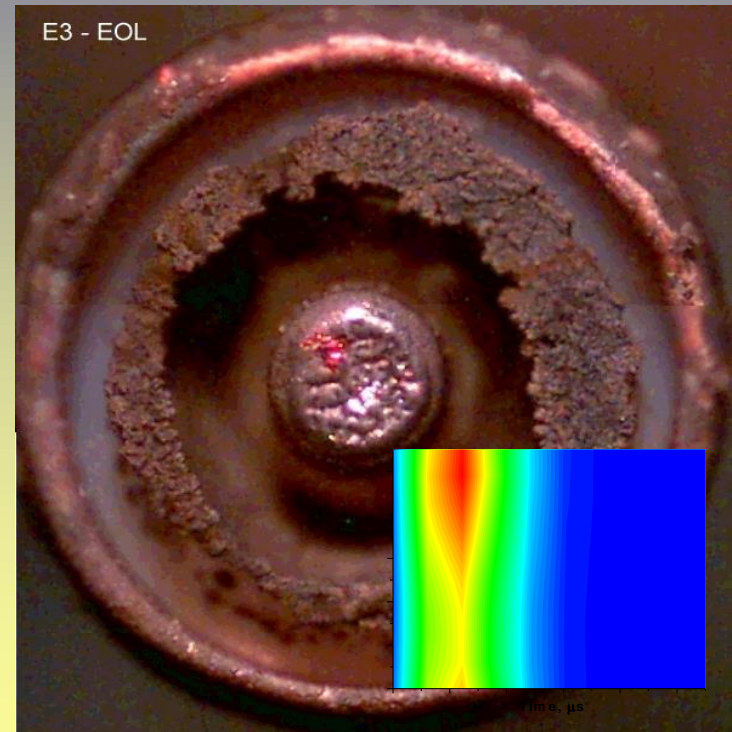
Condition: $kT_2n_2 < kT_1n_1$ and $n_1 > n_2$

If backflux is higher than the primary flux –deposition

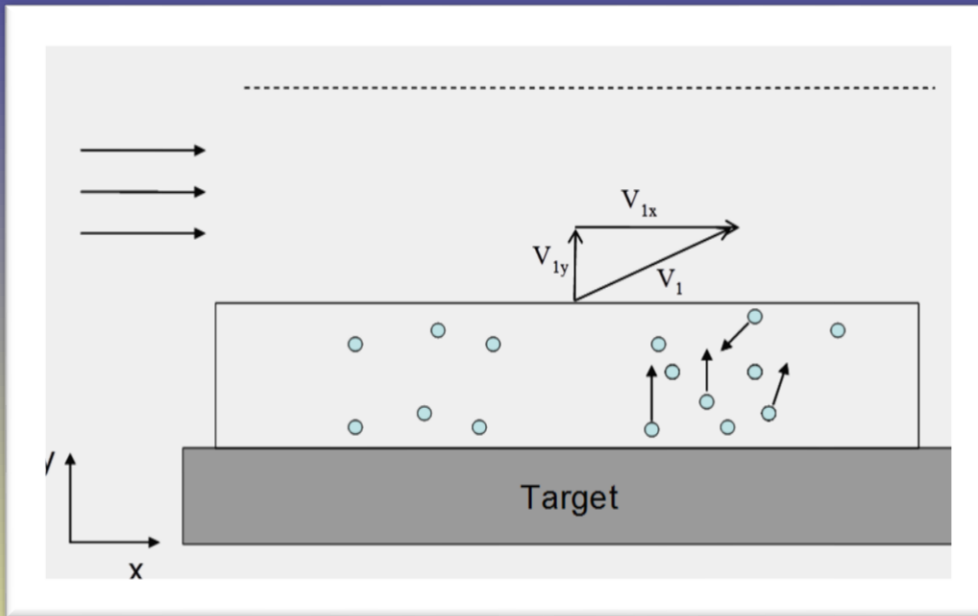
Deposition rate

$$\Gamma = -m(kT_2/m)^{0.5}n_{c2}$$

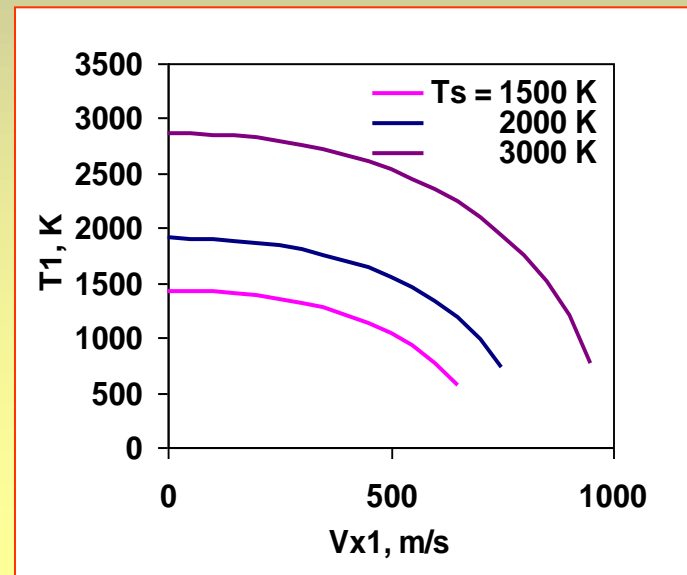
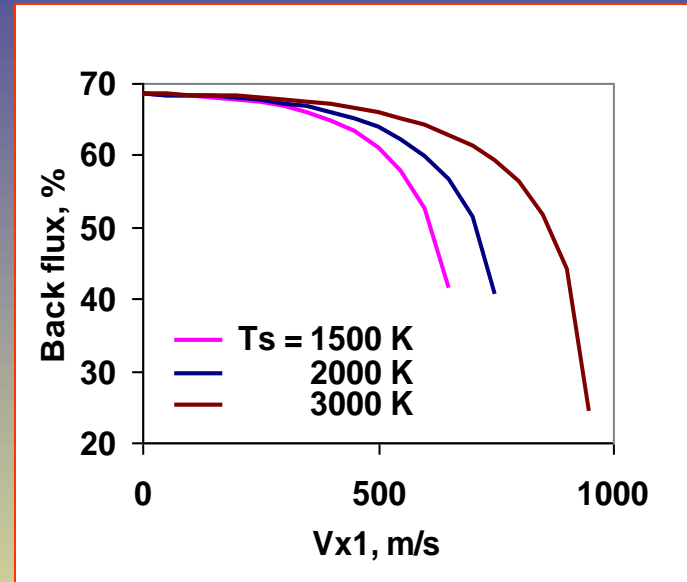
Backflux in Teflon micro-thruster



Effect of cross flow (moving target)

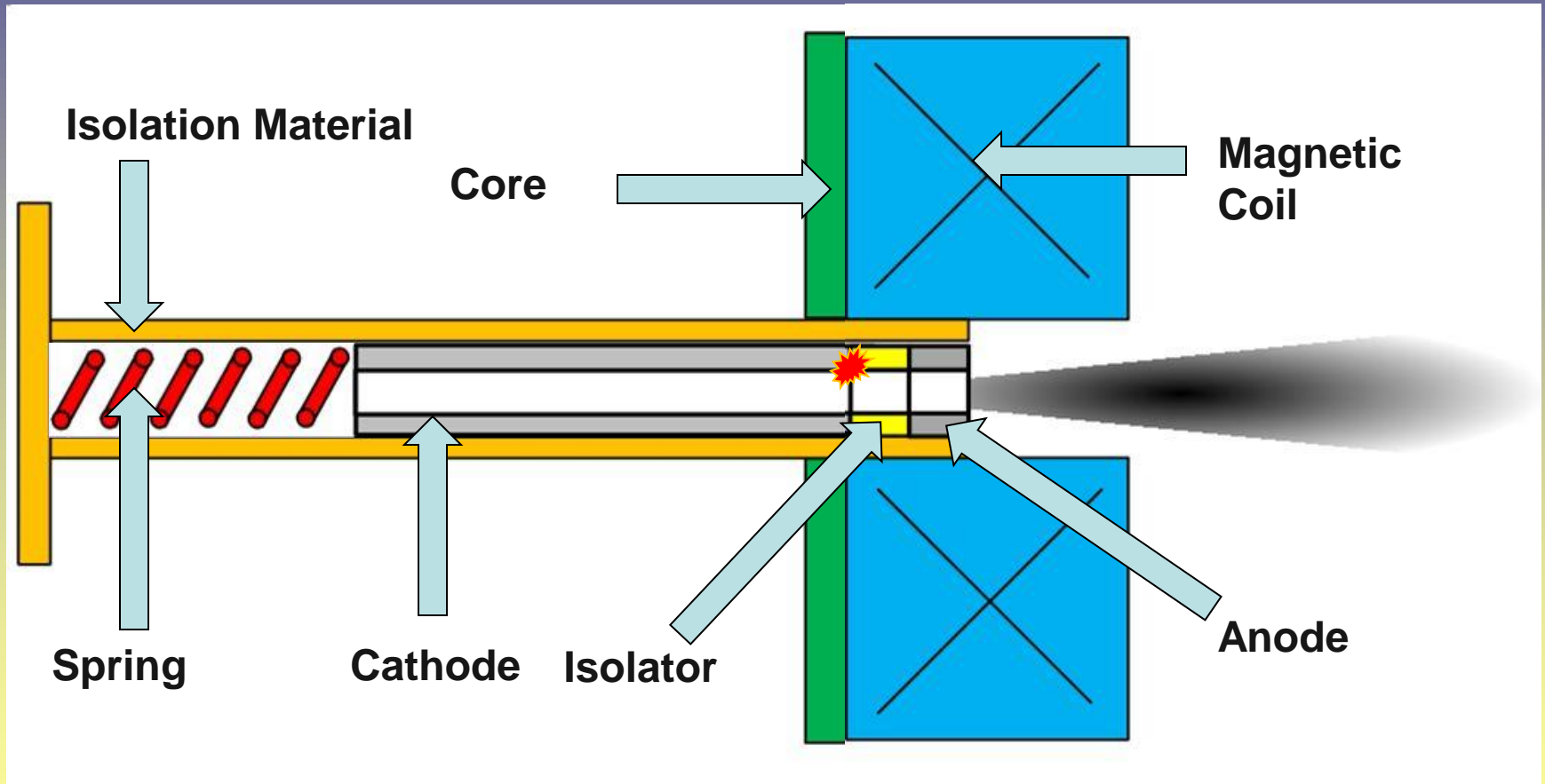


- ❖ Back flux decreases with the increase of cross flow velocity
- ❖ vapor temperature at KL outer edge decreases with the increase of cross flow velocity
- ❖ Ablation rate increases



Micro-Cathode Thruster with Extended Lifetime

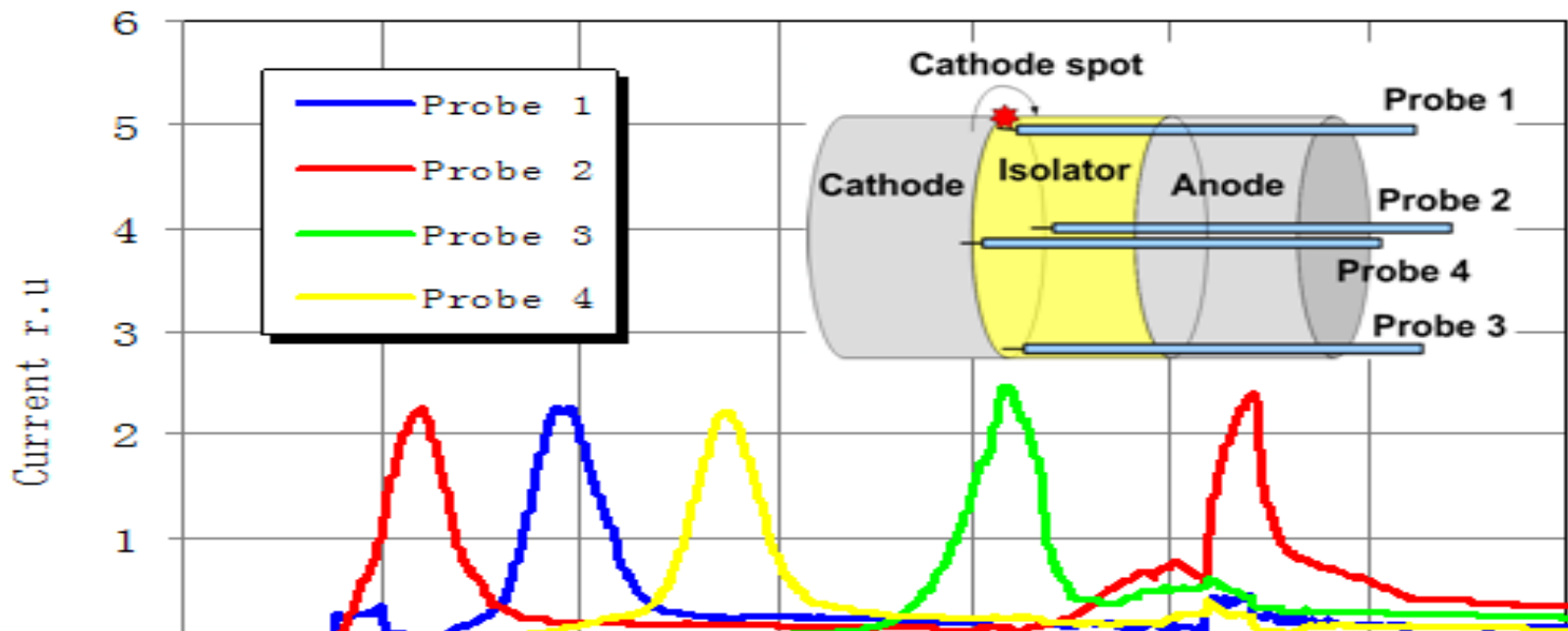
Screened Mechathronics pCT



Micro-cathode arc thruster (μ CAT)

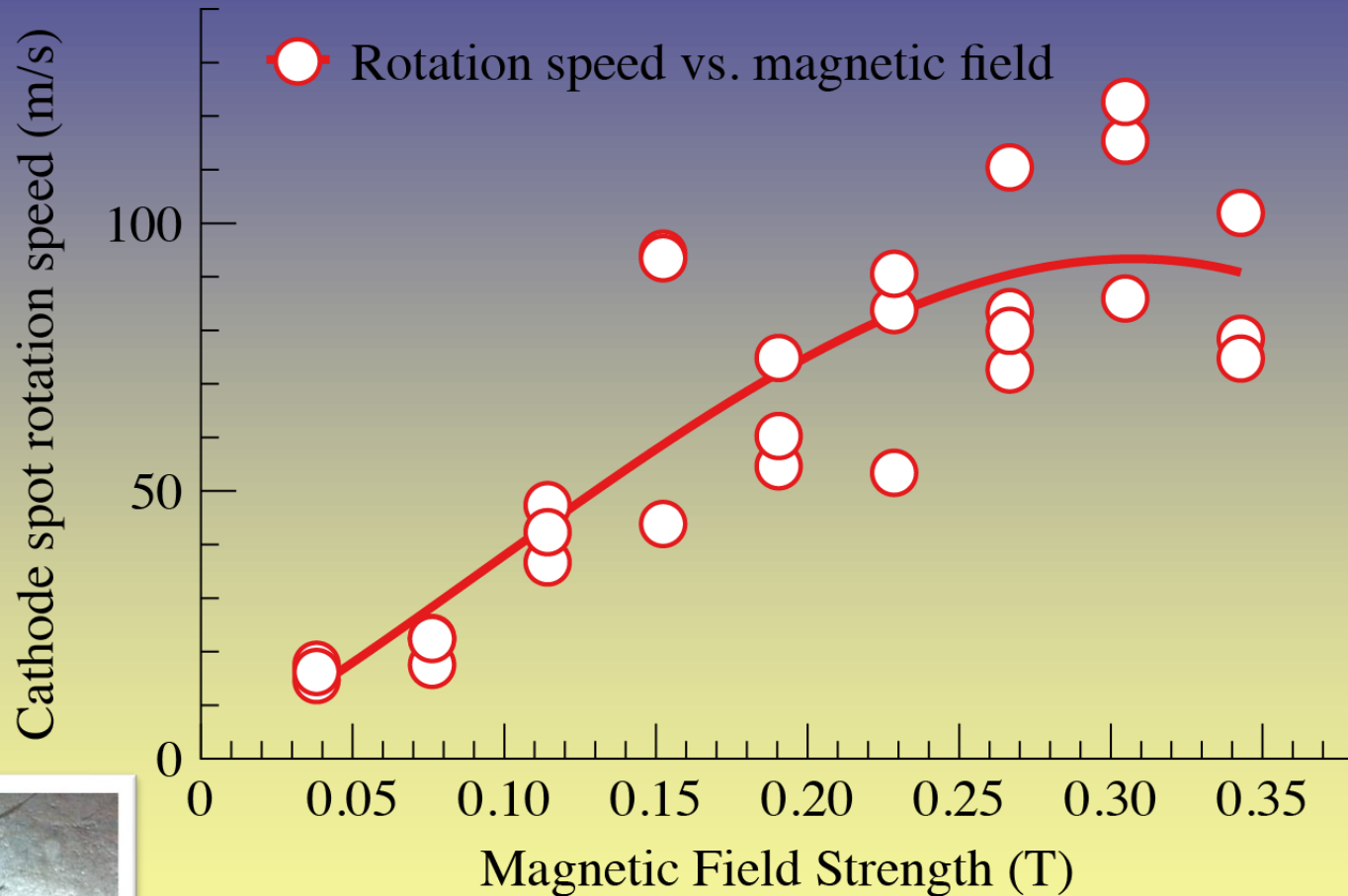


Cathode Spot Rotation

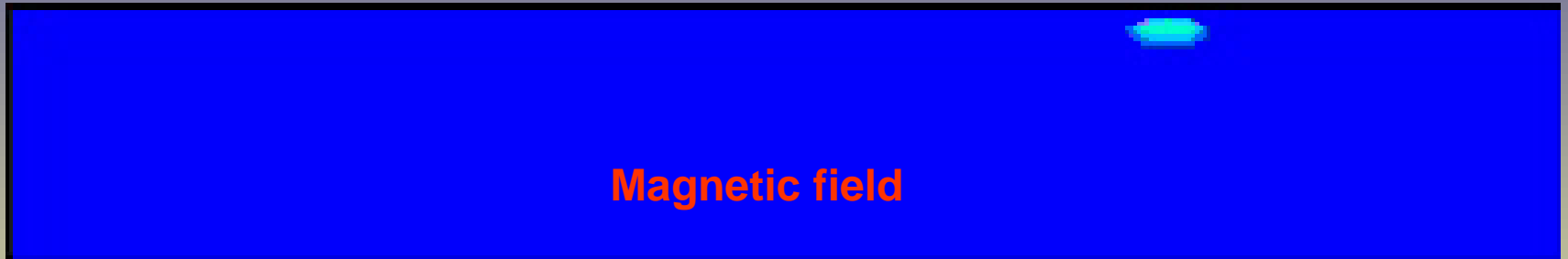


The Experiment Result shown that the Rotation Speed is 75m/s
The Rotation As the Direction of $-J \times B$

Cathode Spot Rotation

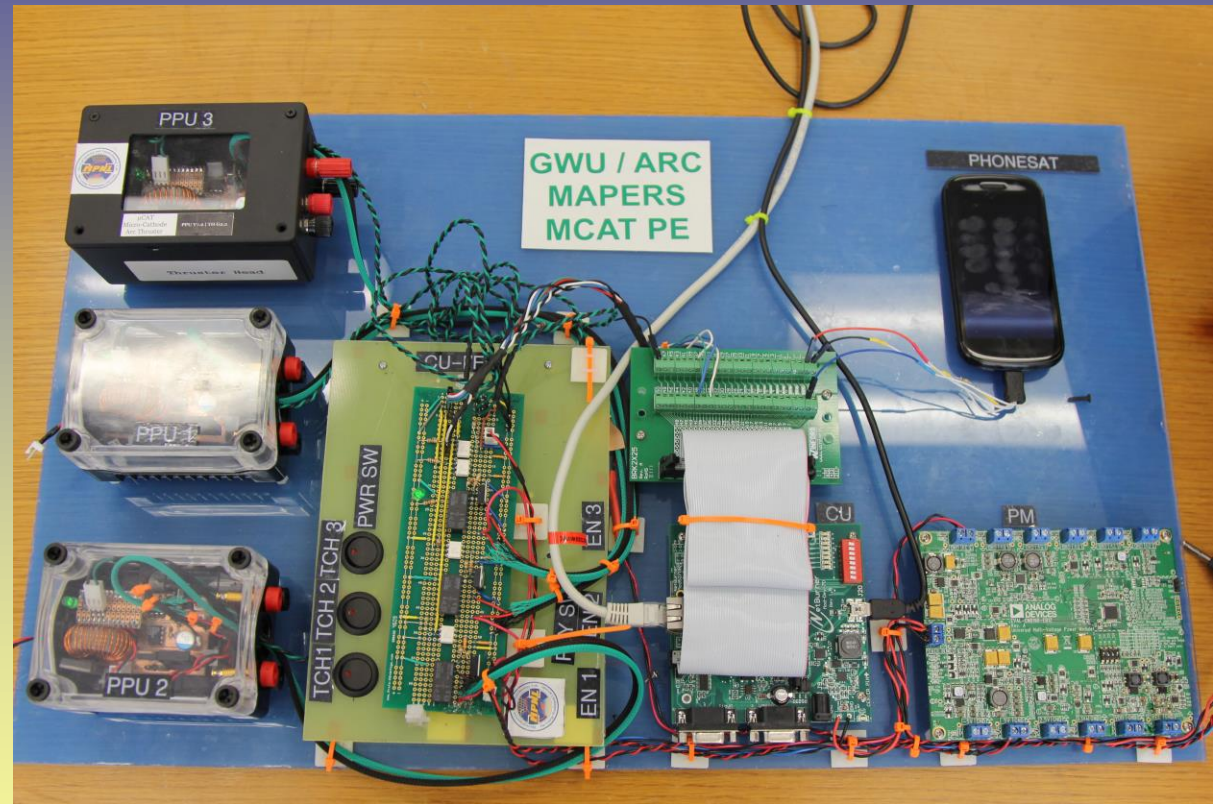


PIC simulations



NASA Ames PhoneSat Experiment

Orbitals' Antares, April 2013

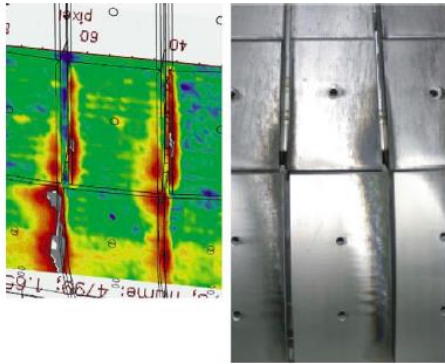


- NASA Ames PhoneSat selected micro-CAT

NASA ARC, August 2013

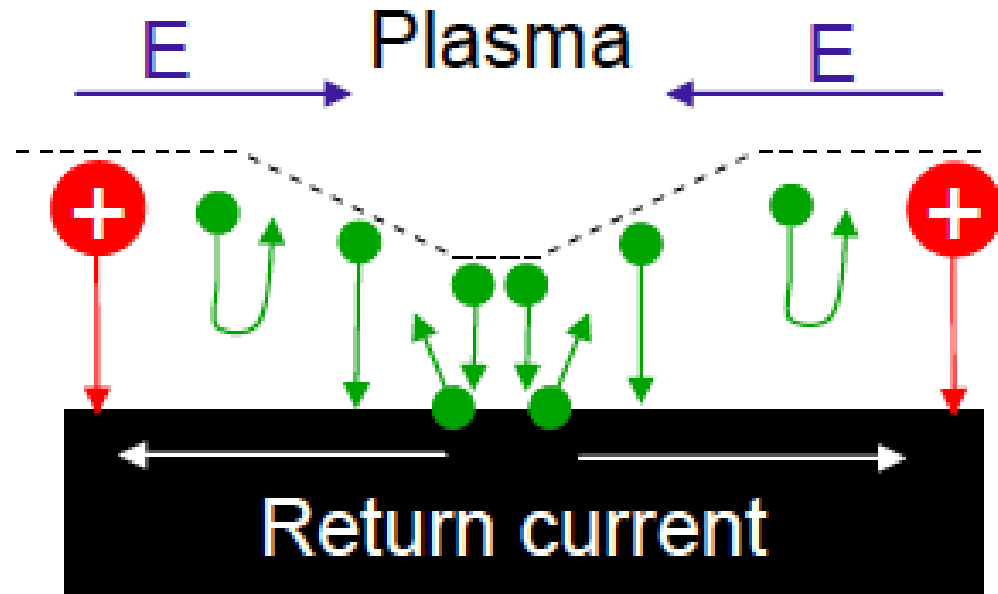
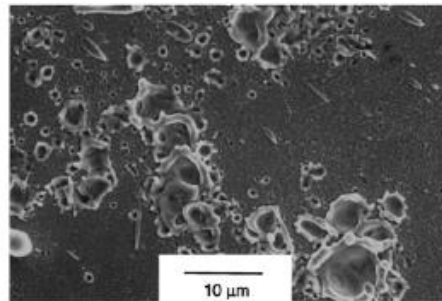
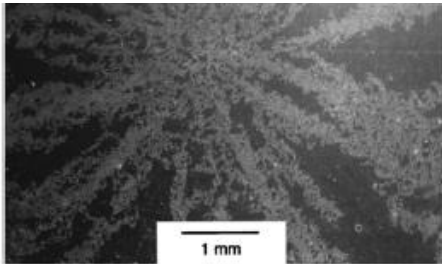
Android app compatible with PhoneSat Bus will be capable of commanding uCATs

Unipolar Arcs



View of the IR-camera and photo of an arc pattern of a comparable region in the inner divertor on ASDEX-Upgrade

A. Herrmann et al., J. Nucl. Materials, 2009

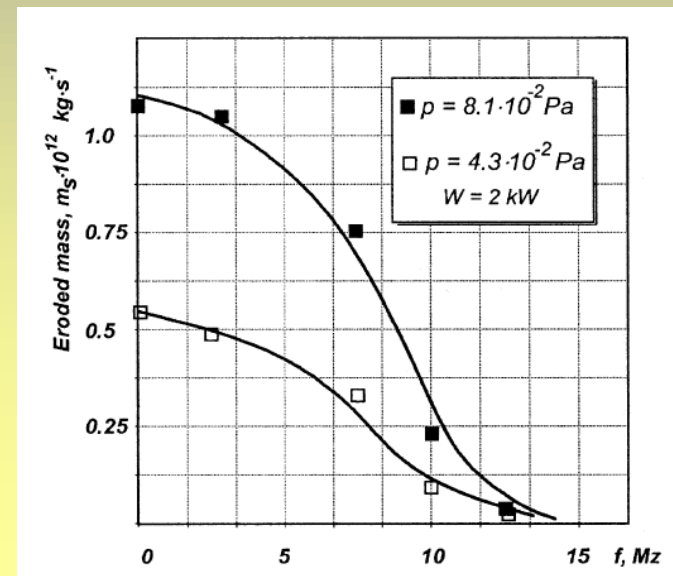
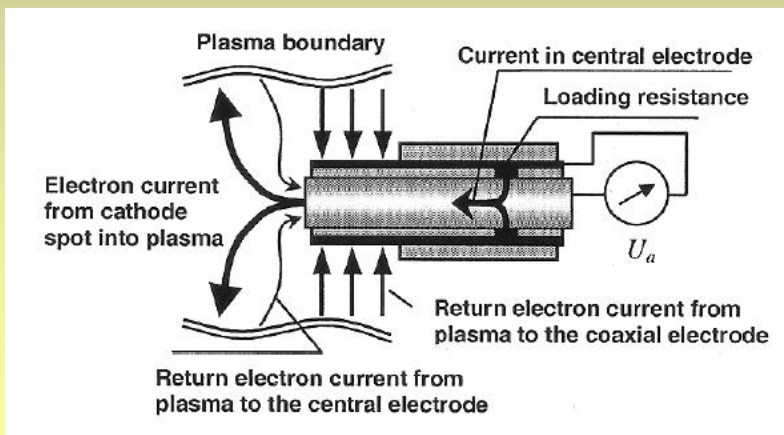
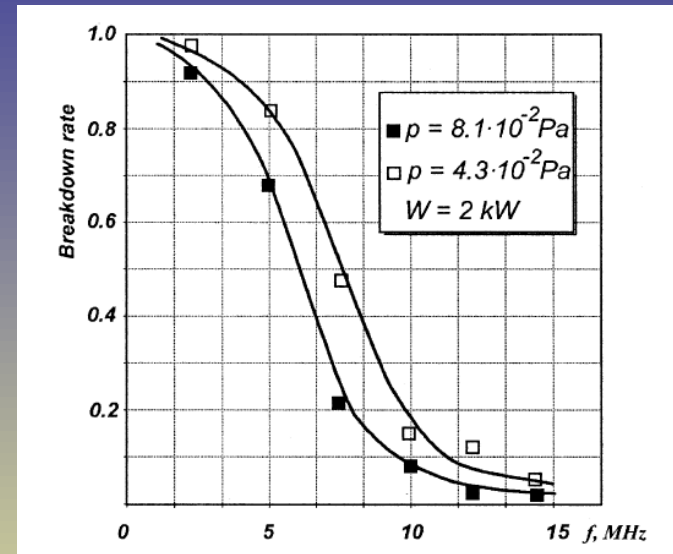
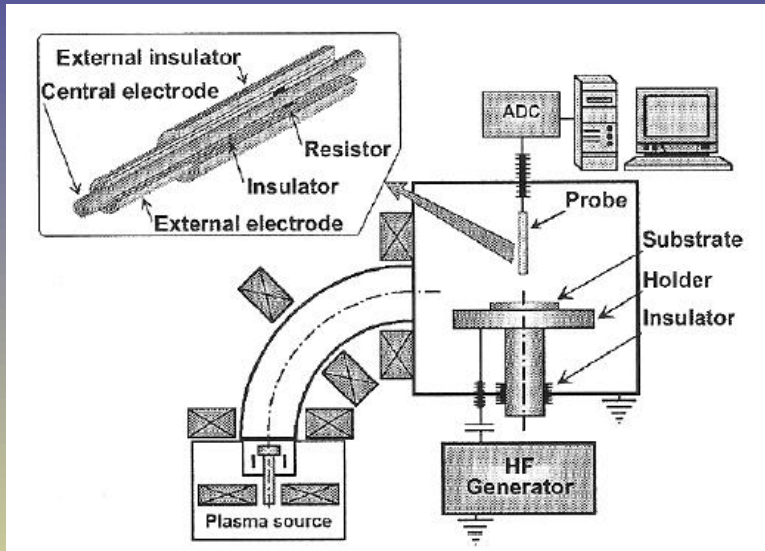


Conductive wall with electron emitting (δ) spot

Global floating condition:

$$\int_s [J_e(1-\delta) - J_i] \cdot dS = 0,$$

Unipolar Arc Suppression



Summary

- Free boundary plasma jet expansion model developed in 90s still useful
- Predicts high-current vacuum arc behavior
- Kinetic erosion model
- Some new devices based on vacuum arcs
- Unipolar arcs suppression



THE GEORGE
WASHINGTON
UNIVERSITY
WASHINGTON, DC



Thank you!

